Automatic Segmentation of the Cervical Region in Colposcopic Images

Paloma Cepeda Andrade, Sesh Commuri
University of Nevada, Reno, 1664 N Virginia St, Reno, NV, U.S.A.

Keywords: Cervical Cancer, Colposcopy, Image Segmentation, LAB Color Space, Morphological Filtering, K-means.

Abstract: Cervical cancer is one of the most common cancers affecting women, especially in developing countries and in resource constrained areas in the western world. While easily treatable if detected early, the lack of adequate resources and skilled physicians make this disease difficult to detect and treat. In this paper, we propose a vision-based approach anchored in machine-learning principles to detect and quantify lesions on the surface of the cervix. Preliminary results indicate that the proposed method can segment images of the cervix and successfully detect lesions other artifacts. The image normalization approach can also determine the locations of lesions and their spread. Validation of this approach during clinical trials is being pursued as the first step towards developing low-cost bioinformatics-based screening tools for early detection of cervical cancer.

1 INTRODUCTION

Cervical cancer is the fourth most frequent cancer in women worldwide and represents 6.6% of all cancers affecting women (WHO, 2019). Most cervical cancer cases are caused by various strains of the Human Papilloma Virus (HPV). There are currently vaccines that protect against common cancer-causing types of HPV and can reduce the risk of cervical cancer.

Cervical cancer is treatable if detected and diagnosed early. Typical screening methods for detecting cervical cancer currently include techniques such as Papanicolau (Pap) smear, HPV typing, and colposcopy. Cost-effective options, such as Visual Inspection with Acetic Acid (VIA), and Visual Inspection with Lugol Iodine (VILI) are recommended as the best screening methods in developing countries (Sankaranarayanan et al., 2003). Cryotherapy or loop electrosurgical excision procedure (LEEP) (Basu & Sankaranarayanan, 2017) can provide effective and appropriate treatment for most women who screen positive for precancerous lesions, and "screen-and-treat" and "screen, diagnose and treat" are both valuable approaches.

Detection of cervical precancerous lesions can be done by examining the cervix, vulva, and vagina through a colposcope. This procedure, called colposcopy, is used to detect genital warts, inflammation of the cervix (cervicitis), and precancerous changes in the tissue of the cervix, vagina, and vulva. During colposcopy, the vaginal walls are held open using a speculum and the surface of the cervix is illuminated using a light source. The colposcope (shown in Figure 1) is then used to visually examine the cervix and the adjacent tissues.

Figure 1: Left: Standard colposcope. Right: Portable colposcope (Basu & Sankaranarayanan, 2017).

During cervical examination, the cervix is first rinsed with saline solution and then stained with 3-5% acetic acid (Sankaranarayanan et al., 2004). If the cervical epithelium contains an abnormal load of cellular proteins, acetic acid causes these proteins to coagulate. As a result, the affected areas appear opaque or white under visual inspection. The higher the grade of neoplasia, the greater the density of acetowhitening (AW) (Li & Poirson, 2006). There are

Andrade, P. and Commuri, S.
Automatic Segmentation of the Cervical Region in Colposcopic Images.
DOI: 10.5220/0010835200003123
In *Proceedings of the 15th International Joint Conference on Biomedical Engineering Systems and Technologies (BIOSTEC 2022) - Volume 1: BIODEVICES*, pages 66-73
ISBN: 978-989-758-552-4; ISSN: 2184-4305
Copyright © 2022 by SCITEPRESS – Science and Technology Publications, Lda. All rights reserved

also other characteristics such as morphological changes (for example, tissue shape, mosaic, and punctuation vessels) that can also indicate abnormalities (Li & Poirson, 2006). Such factors usually require an expert to determine diagnosis.

Abnormal growth of cells on the surface of the cervix if untreated, can potentially lead to cervical cancer. Cervical Intraepithelial Neoplasia (CIN) or Cervical Dysplasia, refers to the potentially precancerous transformation of cells of the cervix. Presence of dysplasia can be further investigated through Pap smear and biopsy. If detected early, CIN can be managed by treatment and full recovery is possible (Castle, Stoler, Solomon, & Schiffman, 2007). However, it is difficult to quantify different characteristics of these lesions unless the patient is examined by a trained professional. Even then, diagnosis can be highly subjective and may lead to misdiagnosis or an unnecessary biopsy (Castle et al., 2007; Kudva & Prasad, 2018).

While screening and treatment has been quite effective in reducing the occurrence of cancer in the developed world, the need for expensive equipment, trained colposcopists, and clinical infrastructure has limited its benefit in other parts of the world. In 2018, around 570,000 women were diagnosed with cervical cancer worldwide, and nearly 311,000 women died from this treatable disease (WHO, 2019). There are many contributing factors to this alarmingly high rate of death. These include social stigma, lack of awareness and access to care, poor staining technique during colposcopy, poor magnification and resolution of the available devices in the market, cumbersome nature of colposcopes due to size and need for electrical power source, and the need for multiple visits to the medical clinics, which can be unpleasant and time-consuming experiences for the patient (WHO, 2019).

Therefore, there is a need for a low-cost and portable tool for screening and detecting abnormal changes in the cervix that may later develop into invasive cancer. Further, the system must be built with automated detection and diagnosis capabilities to enable use by health workers in the field where experienced doctors and colposcopists are not available.

Detection of lesions from images of the cervix has been attempted by several researchers. These approaches utilize digital images of the cervix obtained during colposcopic examination. Staining the cervix with acetic acid exposes any lesions present as white areas (acetowhite regions) under illumination. While these AW regions can be detected, these regions are often distorted by the presence of glare from the light source, reflections from the speculum, as well as portions of the speculum and other artifacts that are captured in the image. Automatic detection of AW regions requires the removal of glare, reflections, and other artefacts from the image, extraction of the region of the cervix that is of interest and detection of the AW regions. Further, it is advantageous to locate the lesion and determine its spread as such information can be used for targeted biopsy instead of the four-quadrant biopsy procedure that is commonly used.

In this paper, we present our approach to detection of precancerous lesions on the cervix. In this approach we first detect glare and specular reflection (SR) in the image. This is followed by image segmentation to identify the cervical region of interest (ROI). The ROI is then used to detect the presence of AW regions that are indicative of lesions. The use of this algorithm in detecting lesions is demonstrated using two colposcopy datasets that are available in the public domain (add references). The method and results are discussed in detail in Sections 3 and 4.

2 LITERATURE REVIEW

2.1 Acquisition of Cervical Images

Automated detection of CIN has benefited from studies over the past several decades where digital images of the cervix were collected. Initial efforts include the Guanacaste Project in Costa Rica between 1993 and 1994 to investigate the role of HPV in the development of CIN (Bratti et al., 2004). In this project, researchers used a fixed-focus camera to obtain cervical images of over ten thousand women. Archived digitized cervical images from this project were later used by Hu and co-researchers to develop a method based on deep learning algorithm for automated visual evaluation of cervical images (Hu et al., 2019).

The ASCUS/LSIL Triage Study for Cervical Cancer (ALTS) was a clinical trial conducted in the United States between 1996 and 2000. ASCUS stands for Atypical Squamous Cells of Undetermined Significance and LSIL for Low-Grade Squamous Intraepithelial Lesions (Schiffman & Adrianza, 2000). The images collected have also been used in several research efforts (Greenspan et al., 2009; Guo et al., 2020) to automate detection of precancerous lesions on the cervix. While these two studies resulted in a wealth of digital images that spurred research into automated analysis of these cervical images, the lack of uniformity in the imaging process, varying light

intensity and focal lengths of the cameras, and varying sizes of the images, make the analysis of these images extremely difficult.

2.2 Detection and Removal of Glare and Specular Reflections (SR)

One of the limiting factors in automatic detection of CIN is the presence of specular reflections in cervical images. The presence of moisture on the surface of the cervix causes reflection of the light source. These reflections, termed as Specular Reflections (SR), appear as bright white spots in the cervigrams and make it difficult to distinguish between AW regions and reflections.

As mentioned in the previous section, staining the cervix with acetic acid can expose potential precancerous lesions. Under normal circumstances, the epithelium remains transparent after the application of acetic acid, but when a precancerous lesion is present, the epithelium becomes opaque, and the reflection of light gives it a white color (Basu & Sankaranarayanan, 2017). An example of this occurrence is shown in Figure 2. The image on the left is of a cervix before the application of acetic acid. The image on the right is of the same cervix, after application of acetic acid, with presence of acetowhite (AW) features. It can also be seen that SR on the cervical image will also appear white in color, but with high brightness and low saturation values. This presents a problem because it can blend in with the AW features of interest and produce incorrect classification or diagnostic results. Therefore, it is necessary to identify these SR areas prior to any medical assessment.

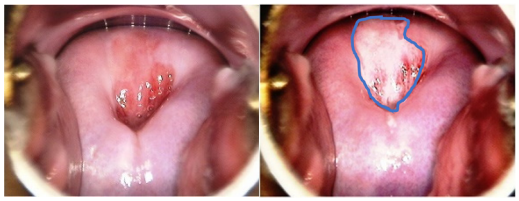

Figure 2: Cervix before (left) and after (right) application of acetic acid. The AW area (blue line) is made visible after applying acetic acid (Basu & Sankaranarayanan, 2017).

Several researchers have attempted to recover information occluded by glare and SR. Lange (Lange, 2005) implemented adaptive thresholding to obtain glare feature maps and remove glare, followed by a filling algorithm to estimate the color and texture in the affected areas. Meslouhi and co-investigators (Meslouhi et al., 2011) proposed an automatic glare extraction and feature inpainting method based on obtaining and comparing luminance components from both RGB and CIE-XYZ color spaces. Das and Bhattarcharyya (Das et al., 2011) developed an algorithm to perform glare removal through the design of morphological filters and with subsequent inpainting using inward interpolation from the pixels outside the detected area. Bai and co-researchers (Bai et al., 2018) also aim to detect areas with SR and restore the area through a filling algorithm.

Region-filling algorithms may provide an estimate of what the area would look like without SR. However, this estimate may forego some texture features that can be of importance in deciding the severity of a precancerous lesion.

2.3 Extraction of the Region of Interest

Color images and the correct representation of features are essential when working with digital medical images. The most common representation of color in images in computer monitors is the sRGB (standard RGB) color space. RGB stands for the three primary colors: red, green, and blue. Images represented in this color space are formed by combining arrays containing values of these individual color components. For most digital images, every possible color can be formed with values in the range of (0, 255) for each primary color component, in the form: $C_i = (R_i , G_i , B_i)$ where $0 \leq R_i , G_i , B_i \leq 255$ (Burger & Burge, 2016). While sRGB is an accepted color standard for screens, it is limited when trying to extract desired features, as there are no light or saturation components, which are good indicators of a lesion present on the cervix.

A different color representation of an sRGB image can make it easier to extract meaningful information. The LAB color space was developed to linearize the representation with respect to human color perception and to generate a more intuitive color space. Color is expressed as three dimensions: L* which represents luminosity; and a* and b*, which are the components that specify hue and saturation along a green-red and blue-yellow axis, respectively (Burger & Burge, 2016). An implementation of this color space to observe a cervical image is illustrated in Figure 3. Note that the L* channel presents information pertaining to the brightness in the image, a useful feature in detecting AW regions.

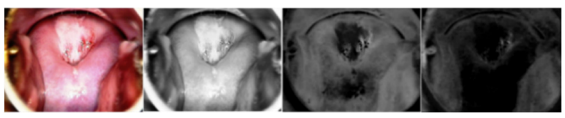

Figure 3: Cervix image converted to CIELAB color space, left to right: Original; L* channel; a*channel; b* channel.

Analysis of a cervical image can be difficult due to the presence of artifacts such as the speculum in the image. These artifacts do not present useful information and are detrimental to the automated detection of lesions. Therefore, detection of the cervical area plays an important role in assessment of colposcopic images by highlighting only the region of interest (ROI). Accurate detection of lesions on a cervix involves removal of glare and SR on the cervical epithelium, accurate delineation of the cervical region, and identification, location, and spread of lesions represented by AW regions.

Figure 4 shows a color image of a cervix. This image contains the speculum used in colposcopy, as well as interference by the reflection of light on the cervical epithelium. Manual delineation of the region of interest and the AW region diagnosed as Cervical Intraepithelial Neoplasia of Grade 1 (CIN1) are also presented.

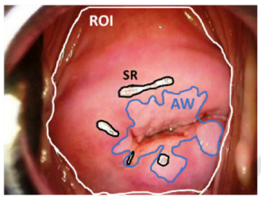

Figure 4: Manual segmentation of the cervical region of interest (ROI), acetowhite staining (AW), and specular reflection (SR).

Several researchers have investigated automatic segmentation of the cervical region to detect lesions. Using hue, saturation, and brightness (HSV color space) information in images, Bai and co-researchers were able to segment cervical images and extract the ROI. Their approach was shown to have accuracy, specificity, and sensitivity of 87.25%, 81.99% and 96.70%, respectively (Bai et al., 2018) Das and Choudhury (Das & Choudhury, 2017) also attempted to obtain the cervical ROI and detect lesions by transforming cervical images into the HSV color space. However, they do not provide validation information to demonstrate that their method can reliably extract the ROI in digital images of the cervix.

Tariq and Burney (Tariq & Burney, 2014) used k-means segmentation to extract the ROI from images of the cervix. In their analysis, they found that k-means ROI segmentation results in better accuracy when images in LAB color space are used in comparison to RGB images. Das and other investigators (Das et al., 2011) proposed an algorithm to detect the cervical ROI and AW lesions using the L* channel of the LAB color space. They achieved accuracy between 89% and 91% but provide no other quantitative metrics to validate their approach.

While these results demonstrate the advantages of using image analysis techniques to study cervigrams, existing results in literature do not adequately address all the challenges in analyzing images of the cervix.

3 METHODS

In this paper, we present a five-step approach to analyzing cervigrams and detecting the presence of lesions on the cervix. These steps are as follows:

1. Convert the cervical image from sRGB to LAB color space and combine the information from the L* and a* channels.
2. Use the k-means algorithm to obtain clusters, segment the image, and identify the cervical ROI.
3. Implement morphological filters to eliminate holes and connect similar regions.
4. Automatically crop the segmented and filtered image to maximize the ROI.
5. Identify AW lesions and calculate their area in proportion to the cervix.

These steps will be further discussed in the next subsections.

3.1 Data Acquisition

We have developed a prototype of the Cervitude Imaging System (CIS). This prototype consists of a probe equipped with a ranging sensor, a camera, and LEDs for illuminating the cervix. The device includes a microprocessor circuit that can control the intensity of the LEDs and provides two-way communication with the CIS application running on a host system such as a computer, Android/iPhone, or a tablet. The CIS application is built around an image analysis algorithm that can quickly detect and locate lesions on the surface of the cervix. With this device, we aim to provide a portable, low-cost, solution to communities that lack the necessary resources and medical personnel. We are currently in the process of performing a clinical study to perform preliminary testing and to obtain our images using this prototype. Two small datasets of cervical images that are available online were used to demonstrate the algorithms presented in this paper.

The first dataset used was obtained through the Atlas of Colposcopy (Basu & Sankaranarayanan). The Atlas of Colposcopy was developed by the International Agency for Research on Cancer (IARC)

and provides detailed information on everything related to colposcopy. It is designed to serve as a comprehensive manual for anyone working in this area, both in the medical field and academic research. This website contains a small repository of images (107 in total) labeled in order of severity, from "Normal" to "CIN-1", "CIN-2", "CIN-3", and "Carcinoma in situ (CIS)". These images are of relatively high quality, with a size of 600 x 800 pixels, which makes them suitable for the segmentation approach presented in this paper. The main drawback is that there are no annotations available regarding the cervical ROI, so a qualitative evaluation on the segmentation results will be made.

The next image dataset that was used for analysis is publicly available online[1] by Fernandes and co-researchers (Fernandes et al., 2017). This dataset contains a total of 284 colposcopic images with annotations for the cervical ROI. Out of these, we will use 91 images, which represent the cervical region after acetic acid has been used. The annotations provided will be used to validate our segmentation algorithm. However, a downside is that there is no pathological information available, so AW lesion segmentation cannot be validated with this dataset.

3.2 Image Pre-processing

Our image pre-processing approach addresses the challenges in cervical image analysis in the following ways: by identifying regions containing SR, and by preparing the image for k-means segmentation through conversion of the images to LAB color space. From Figure 3, it can be observed that both the L* and a* channels can provide meaningful information. Therefore, this method uses the information obtained after combining these two channels, as they will bring out the areas that present a high level of brightness and absence of pink or red colors. The results of combining these two channels are shown on Figure 5.

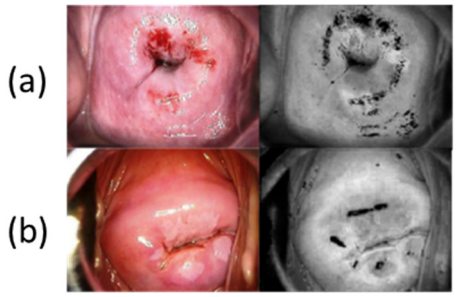

Figure 5: Visualization of the combination of L* and a* channels. Left: original images. Right: resulting images.

[1] https://archive.ics.uci.edu/ml/datasets

The results from Figure 5 show a way to interpret specular reflections as an undesired feature for diagnosing a precancerous lesion. Image (a) is that of a healthy cervix, so correctly detecting these natural features is essential to avoid over-treating a patient for a misdiagnosed illness. Similarly, image (b) shows the correct identification of areas with SR, while leaving out the AW region.

3.3 Segmentation of the Cervical Region

Image segmentation is a critical step when processing images for classification. Through this process, an image can be split into a given number of regions. The k-means algorithm is a type of unsupervised clustering algorithm commonly used for image segmentation (Luo et al., 2003) due to its simplicity and speed. It divides a dataset (in this case, an image) into *K* classes, such that similar regions are clustered together. The objective is to find the center of each cluster C_i and to assign all sample points in the vicinity of the center to that cluster (Tariq & Burney, 2014).

The center of each cluster is the mean of the data points which belong to it. A Euclidean distance measurement:

$$D(x, y) = \|x - y\| \quad (1)$$

is used to determine which cluster a data point belongs to. The algorithm works as follows:

1. For a given number of K, the data points are randomly grouped into each cluster.
2. The center of each cluster is calculated.
3. The distance from each point to each cluster center is calculated.
4. Each point is reassigned to the nearest cluster.

Steps 2-4 are repeated iteratively until there are no changes in the grouping.

The input to our k-means segmentation algorithm is the image resulting from the element-wise multiplication of the L* and a* channels. Then, we implement the k-means algorithm to obtain three clusters. Finally, we implement morphological filtering using a hole-filling operation, followed by an opening operation, which removes small dark spots on the image, and connects the bigger, white, areas. In most cases, this will leave our resulting binary mask, which will indicate the cervical ROI. In a few

cases, two or more resulting areas will appear. If that occurs, the largest area will be considered as the ROI.

4 RESULTS AND DISCUSSION

4.1 Atlas of Colposcopy Dataset

Figure 6 shows the segmentation results on the Atlas of Colposcopy dataset. The first column shows the original RGB colposcopy image. The second column displays the resulting outline after LAB color space conversion and our segmentation algorithm. The third column represents the segmented colposcopic image, without the speculum and outer edges of the cervical region.

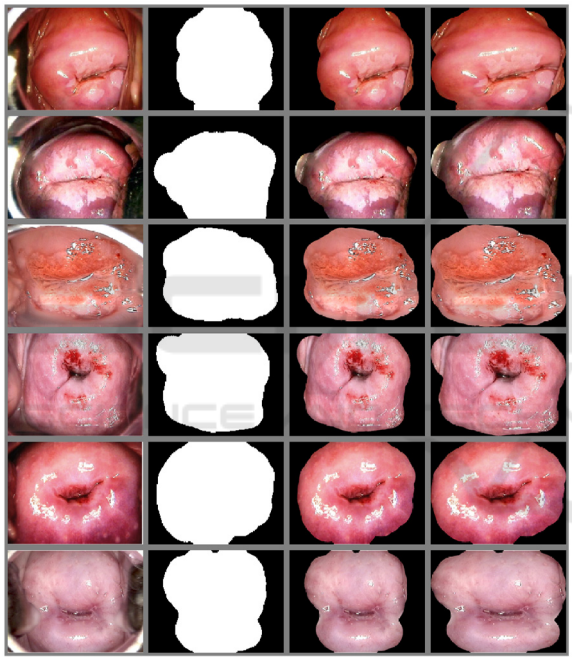

Figure 6: ROI Segmentation Results. Left to right: Original image; binary mask; segmented image; cropped and resized segmented image.

Additionally, an auto-crop function was created to ensure that the cervical area remains at the center of the processed image. The results are shown on the fourth column in Figure 6. If the image is rotated, the region of interest will remain at the center. An example is illustrated in Figure 7. The size of the segmented and cropped image is 486 x 599 pixels.

To detect the presence of AW lesions, the k-means algorithm was used to perform automatic segmentation of the image in Figure 7. The image represents a cervix with CIN 2, where a portion of the cervix is covered by AW lesions. Without the presence of the speculum and the background, the AW region detection was successful. The result is shown on Figure 8.

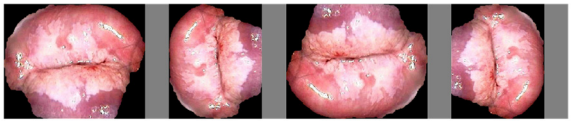

Figure 7: Segmentation and auto-cropping of cervical image after 90-degree rotation.

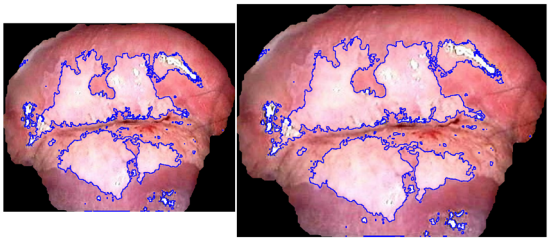

Figure 8: AW lesion detection results. Left: Cropped image. Right: Cropped and resized image.

From Figure 8, the area of the identified AW regions in the cropped image covers 35.39% of the cervical ROI. When the image is resized to its original dimensions, the segmentation algorithm detects that the AW area covers 35.34% of the cervical ROI. This shows that when the cropped and segmented image is resized to the original dimensions, the AW area proportion remains within algorithmic precision.

This shows that the ROI segmentation and auto-cropping will retain the same ratio of AW region with respect to the area of the cervix. The process is almost unaffected by the size and orientation of the original image. Therefore, the procedure can be used during cervical screening using portable colposcopes or other imaging devices. Further, the procedure affords a simple way to compare screening results from several patient visits and can be used to document the efficacy of the treatment regimen.

4.2 Fernandes Dataset

We also performed our ROI segmentation algorithm on the images from the Fernandes dataset. Figure 9 shows our results compared to the provided annotations. The first column contains the original images, the second column shows our segmentation results with true negative values in black, true positive values in white, false negative values in blue, and false positive values in red. The third column shows the ground truth annotations, and the fourth column shows the final, segmented image.

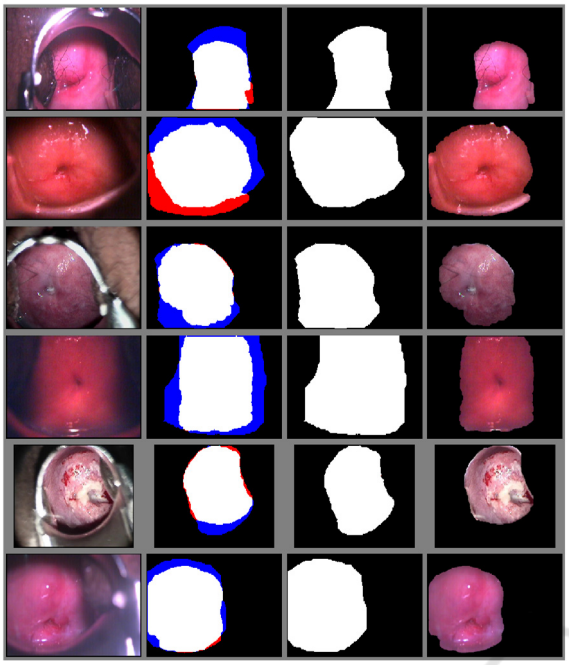

Figure 9: ROI Segmentation Results. Left to right: Original image; binary mask with false negative segmentation in blue, and false positive segmentation in red; ground truth; segmented image.

The false negative (FN) values are those which are annotated as cervix, and which our algorithm classified as non-cervix. While we consider this dataset to be of relatively good quality, in many cases the illumination in the images is not adequate, and shadows present in them can affect the performance of our algorithm. We observed that most of our errors are FN, where our algorithm did not include shadowed areas in the cervix as part of the ROI. Even though we do not have annotations in our other dataset, a qualitative assessment of our results indicates that if the ROI is well illuminated, our FN rate will go down.

The quantitative evaluation of our algorithm is shown in Table 1. Our results show that the average accuracy of the segmentation algorithm was 83.33%. In fact, 67 out of 91 images were segmented with accuracy over 80%. Specificity indicates the proportion at which our algorithm can classify pixels that are not part of the ROI. The average specificity was almost 87%. Our average sensitivity is about 81%, which shows the rate at which we can correctly identify a pixel as part of the ROI. Precision is the measurement indicating the possibility that the pixel classified as part of the cervix is not part of the background (Gerig et al., 2001). The average precision is 80.53%.

Table 1: Accuracy and performance of our segmentation algorithm.

Performance Metric	Max (%)	Min (%)	Median (%)	Mean (%)
F1 Score	95.50	47.36	82.07	79.46
Accuracy	97.44	58.32	83.84	83.33
Specificity	100	58.77	88.83	86.63
Sensitivity	99.72	33.24	81.58	81.12
Precision	100	42.82	81.73	80.53

Our experimental results show that our segmentation algorithm performs in a suitable manner, with accuracy, specificity, and sensitivity of up to 97.44%, 100%, and 99.72%, respectively. This means that the algorithm can segment the cervical region in clinical practice with excellent results. We have shown that, given a small amount of data, an algorithm can be developed to identify the cervical ROI, regardless of position or distance from the colposcope to the cervix. Further improvements are expected as we complete our clinical study.

5 CONCLUSIONS

In this paper, an image analysis-based approach for screening for cervical cancer was presented. Preliminary results indicate that the proposed method can segment images of the cervix, reduce the effect of glare from light sources, remove specular reflections and other artifacts, and successfully detect lesions. While the method was validated using sample images from the Atlas of Colposcopy and the Fernandes dataset, extensive analysis must be conducted using a variety of images collected in the field to improve the sensitivity and specificity of the method in obtaining the cervical ROI and detecting cervical dysplasia.

Validation of this approach during clinical trials is being pursued by the authors as the first step towards developing low-cost bioinformatics-based screening tools for early detection of cervical cancer. Accurate automatic detection of cervical dysplasia can prove to be crucial in regions where medical experts or clinical resources are not available.

REFERENCES

(WHO), W. H. O. (2019). *Cervical Cancer*. https://www.who.int/cancer/prevention/diagnosis-screening/cervical-cancer/en/

Bai, B., Liu, P. Z., Du, Y. Z., & Luo, Y. M. (2018). Automatic segmentation of cervical region in colposcopic images using K-means. *Australas Phys Eng Sci Med*, *41*(4), 1077-1085. https://doi.org/10.1007/s13246-018-0678-z

Basu, P., & Sankaranarayanan, R. (2017). *Atlas of Colposcopy – Principles and Practice*. IARC CancerBase. https://screening.iarc.fr/atlascolpo.php

Bratti, M. C., Rodríguez, A. C., Schiffman, M., Hildesheim, A., Morales, J., Alfaro, M., Herrero, R. (2004). Description of a seven-year prospective study of human papillomavirus infection and cervical neoplasia among 10000 women in Guanacaste, Costa Rica, *Rev Panam Salud Publica*, *15*(2), 75-89. https://doi.org/10.1590/s1020-49892004000200002

Burger, W., & Burge, M. J. (2016). *Digital Image Processing* (2 ed.). Springer-Verlag London. https://doi.org/10.1007/978-1-4471-6684-9

Castle, P. E., Stoler, M. H., Solomon, D., & Schiffman, M. (2007). The relationship of community biopsy-diagnosed cervical intraepithelial neoplasia grade 2 to the quality control pathology-reviewed diagnoses: an ALTS report. *Am J Clin Pathol*, *127*(5), 805-815. https://doi.org/10.1309/PT3PNC1QL2F4D2VL

Das, A., Avijit, K., & Bhattacharyya, D. (2011). *Elimination of specular reflection and identification of ROI: The first step in automated detection of Cervical Cancer using Digital Colposcopy* 2011 IEEE International Conference on Imaging Systems and Techniques.

Das, A., & Choudhury, A. (2017). A novel humanitarian technology for early detection of cervical neoplasia: ROI extraction and SR detection. 2017 IEEE Region 10 Humanitarian Technology Conference (R10-HTC), Dhaka.

Fernandes, K., Cardoso, J. S., & Fernandes, J. (2017). Transfer Learning with Partial Observability Applied to Cervical Cancer Screening. In L. A. Alexandre, J. Salvador Sánchez, & J. M. F. Rodrigues, *Pattern Recognition and Image Analysis* Cham.

Gerig, G., Jomier, M., & Chakos, M. (2001). Valmet: A New Validation Tool for Assessing and Improving 3D Object Segmentation. In W. J. Niessen & M. A. Viergever, *Medical Image Computing and Computer-Assisted Intervention – MICCAI 2001* Berlin, Heidelberg.

Greenspan, H., Gordon, S., Zimmerman, G., Lotenberg, S., Jeronimo, J., Antani, S., & Long, R. (2009). Automatic detection of anatomical landmarks in uterine cervix images. *IEEE Trans Med Imaging*, *28*(3), 454-468. https://doi.org/10.1109/TMI.2008.2007823

Guo, P., Xue, Z., Long, L. R., & Antani, S. (2020). Cross-Dataset Evaluation of Deep Learning Networks for Uterine Cervix Segmentation. *Diagnostics (Basel)*, *10*(1).

Hu, L., Bell, D., Antani, S., Xue, Z., Yu, K., Horning, M. P., Schiffman, M. (2019). An Observational Study of Deep Learning and Automated Evaluation of Cervical Images for Cancer Screening. *J Natl Cancer Inst*, *111*(9), 923-932. https://doi.org/10.1093/jnci/djy225

Kudva, V., & Prasad, K. (2018). Pattern Classification of Images from Acetic Acid-Based Cervical Cancer Screening: A Review. *Crit Rev Biomed Eng*, *46*(2), 117-133. https://doi.org/10.1615/CritRevBiomedEng.2018026017

Lange, H. (2005). Automatic glare removal in reflectance imagery of the uterine cervix. Proceedings of SPIE - The International Society for Optical Engineering,

Li, W., & Poirson, A. (2006). Detection and Characterization of Abnormal Vascular Patterns in Automated Cervical Image Analysis. In G. Bebis, R. Boyle, B. Parvin, D. Koracin, P. Remagnino, A. Nefian, G. Meenakshisundaram, V. Pascucci, J. Zara, J. Molineros, H. Theisel, & T. Malzbender, *Advances in Visual Computing* Berlin, Heidelberg.

Luo, M., Ma, Y.-F., & Zhang, H.-J. (2003). *A Spatial Constrained K-means A pproach to Image Segmentation* Joint Conference of the Fourth International Conference on Information, Communications and Signal Processing, 2003 and Fourth Pacific Rim Conference on Multimedia Singapore.

Meslouhi, O., Kardouchi, M., Allali, H., Gadi, T., & Benkaddour, Y. (2011). Automatic detection and inpainting of specular reflections for colposcopic images. *Open Computer Science*, *1*(3).

Sankaranarayanan, R., Shastri, S. S., Basu, P., Mahé, C., Mandal, R., Amin, G., Dinshaw, K. (2004). The role of low-level magnification in visual inspection with acetic acid for the early detection of cervical neoplasia. *Cancer Detect Prev*, *28*(5), 345-351. https://doi.org/10.1016/j.cdp.2004.04.004

Sankaranarayanan, R., Wesley, R., Thara, S., Dhakad, N., Chandralekha, B., Sebastian, P., Nair, M. K. (2003). Test characteristics of visual inspection with 4% acetic acid (VIA) and Lugol's iodine (VILI) in cervical cancer screening in Kerala, India. *Int J Cancer*, *106*(3), 404-408. https://doi.org/10.1002/ijc.11245

Schiffman, M., & Adrianza, M. E. (2000). ASCUS-LSIL Triage Study. Design, methods and characteristics of trial participants. *Acta Cytol*, *44*(5), 726-742. https://doi.org/10.1159/000328554

Tariq, H., & Burney, S. M. A. (2014). K-Means Cluster Analysis for Image Segmentation. *International Journal of Computer Applications*, *96*.